Annals of Nuclear Energy 136 (2020) 106992

Contents lists available at ScienceDirect

Annals of Nuclear Energy

journal homepage: www.elsevier.com/locate/anucene

Technical note

Improvements of subgroup method based on fine group slowing-down calculation for resonance self-shielding treatment

Song Li, Zhijian Zhang *, Qian Zhang *, Qiang Zhao

Fundamental Science on Nuclear Safety and Simulation Technology Laboratory, College of Nuclear Science and Technology, Harbin Engineering University, Harbin 150001, China

ARTICLE INFO

Article history:
Received 28 May 2019
Received in revised form 29 June 2019
Accepted 14 August 2019
Available online 16 September 2019

Keywords:
Resonance self-shielding
Subgroup method
Ultra-fine group method
Resonance interference effect

ABSTRACT

To combine the advantages of the accuracy of ultra-fine group method and efficiency of subgroup method for resonance self-shielding treatment, the method of fine-mesh subgroup method (FSM) has been raised in this paper. FSM adopts a fine energy mesh of 289 groups for resonance energy range and the subgroup parameters are generated for each group. The Coupling procedure ensures the elimination of extra resonance interference amendment as the group structure is sufficient enough. To improve the efficiency, the micro level optimization based on "one-group" approximation is proposed to solve the subgroup fixed source equations for only 8 subgroup levels for each resonant nuclide. Finally, a group condense procedure based on neutron slowing-down equation is employed for resonance range from 289 to 16 groups, and a 47-group structure library will be used for eigenvalue calculation. Benchmarks of pin cells and lattices in reactors are applied in numerical validation and the calculating results show that FSM has a good performance with both accuracy and efficiency for complicated resonance treatment.

1. Introduction

Resonance self-shielding treatment is one of the most dominant procedures of numerical simulation for reactor physics as it provides effective cross sections for the whole process. However, due to the severe fluctuation of resonance cross sections and resonance interference effect, handling resonance self-shielding effect accurately and efficiently becomes very difficult to achieve, especially under conditions like burn-up or complicated fuel material compositions. With the development of computational technology, application of the deterministic approach to describe the physical phenomenon in reactor becomes the mainstream (Cacuci, 2010). Deterministic calculating method for resonance self-shielding treatment has also become one of the research hotspots.

Traditional deterministic methods for self-shielding calculation include equivalence theory (Askew et al., 1966; Hebert and Marleau, 1991), ultra-fine group method (Ishiguro and Takano, 1971; Sugimura and Yamamoto, 2007; Zhang et al., 2018a) and subgroup method (Nikolaev et al., 1971; Cullen, 1977; Hebert, 2009a; Downar et al., 2016). Equivalence theory establishes a correspondent relationship of equivalence between homogeneous and heterogeneous problems, and the key part of this method is to capture the escape probability from absorption. Equivalence theory has been adopted by programs like WIMS (Powney and Newton, 2004), CASMO (Rhodes et al., 2006), and APOLLO (Cacuci, 2010). It is simple and fast, but has an obvious inability to handle complicated geometry and space dependent self-shielding effect. Ultra-fine group method was developed in the early time of reactor physics calculation, which evaluates resonance cross sections by an extremely fine energy mesh. As the variation trend of resonance has been described in detail like continuous energy, cross sections can be produced very accurately and no extra resonance interference correction is needed. Programs like PEACO (Ishiguro and Takano, 1971) and AEGIS (Sugimura and Yamamoto, 2007) are based on this method. However, as the ultra-fine group transport calculation has a high usage for computation time and memory resource, this method could only be used in single pin cell or small scale lattice. Unlike the conventional method, subgroup method divides the neutron group by the magnitude of the value of cross section other than energy, and the fluctuation of flux, which could be deduced by subgroup parameters, is gentle enough to be considered as constant in a subgroup. In this way, only a few further subdivision of subgroups in a conventional resonance group can result in the similar accuracy as thousands of ultra-fine groups. Furthermore, subgroup method can be combined with any kind of transport method to solve subgroup fixed source problems, which makes it possible to treat any kind of geometry. Due to the relatively high accuracy and adaptability, subgroup method has been

* Corresponding authors.
E-mail addresses: zhangzhijian_heu@hrbeu.edu.cn (Z. Zhang), qianzhang@hrbeu.edu.cn (Q. Zhang).

https://doi.org/10.1016/j.anucene.2019.106992
0306-4549/

applied into many programs like HELIOS (Stamm'ler, 2008), MPACT (Kochunas et al., 2013), DeCART (Joo et al., 2004), nTRACER (Jung et al., 2013) and NECP-X (Chen et al., 2018). Nevertheless, subgroup method still needs the correction calculation for resonance interference effect, such as Bondarenko iteration method (BIM) (Askew et al., 1966) and resonance interference fact method (RIFM) (Williams, 1983; Park et al., 2017), which usually accounts for the most time consuming part of resonance calculation. In recent years, there are other newly proposed method like embedded self-shielding method (ESSM) (Zhang et al., 2015; Liu et al., 2015), pseudo resonant isotope method (PRIM) (Zhang et al., 2018b,c; Liu et al., 2018), pin-based pointwise energy slowing-down method (PSM) (Choi et al., 2017) and so on. The accuracy of these methods are satisfying but they treat the fuel pin as a whole object, so the resonance in sub-pin level still needs the extra correction method like spatial dependent Dancoff method (SDDM) (Matsumoto et al., 2005) and so on.

From the current existing calculation method, it can be found that a promising approach by combing the accuracy of ultra-fine group method with the efficiency and geometry adaptability of subgroup method, and an equilibrium point could be found between computational burden and precision. To achieve the prospective above, the fine-mesh subgroup method (FSM), which is based on the coupling method between subgroup and ultra-fine group is raised in this work. First, to capture the self-shielding behavior of different resonant isotopes, a finer mesh should be adopted. As the subgroups also account for a further division for the coarse resonance group, the new fine mesh does not need to be the same energy density as ultra-fine group, so a 289-groups structure from 1.8554 eV to 9118 eV is finally selected. Subgroup parameters are generated in each group by the fitting method (Hebert, 2009b), which is based on the resonance integrals in the homogeneous problem. In this work, the NJOY program (Macfarlane et al., 2016) is applied to provide the multi-group data for both fine mesh structure and condensed mesh structure afterward. However, although a finer mesh could save plenty of time by avoiding resonance interference treatment, the increment of the number of resonance groups inevitably results in the sharp rise of calculating time for subgroup fixed source equations, which is unacceptable compared with the traditional subgroup method. To handle this problem, the micro level optimization is proposed in this paper. As the subgroup flux could be obtained by interpolation (Stamm'ler, 2008; Park and Joo, 2018), it is not necessary to solve the subgroup fixed source equations for every subgroup level. Moreover, it can be seen that the value of the source item in subgroup fixed source equations for a certain nuclide is also close in different group, so a group-averaged fixed source could be defined to use in all groups. In this way, subgroup fixed source equations are only needed to be solved in an averaged "one-group" by a certain set of subgroup levels respectively. In this work, a set of 8 micro subgroup levels from 10 bar to 10^5 bar is selected for one-group subgroup fixed source problems. This procedure significantly reduces the computational burden compared with traditional subgroup method which usually needs several dozens of levels in total for each resonant nuclide. In addition, as the finer mesh will also cause a substantial increase of resource usage in the transport module, a group condensation scheme is also needed after the resonance calculation. In this work, the 289-groups structure for resonance energy range is used first to deal with the self-shielding effect. Subsequently, the slowing down equations for 289 groups are solved to get the fluxes for group condensation of effective cross sections. The condensed group structure adopts the 47-groups structure with 16 resonance groups (Kim et al., 2015) for eigenvalue calculation. For resonance groups, the fission source and up-scattering effect can be neglected so that the source item only consist of down-scattering effect. Once the fluxes of the groups with higher energy are known, the slowing down equation will become a one-group fixed source problem. In addition, for down-scattering source from the fast group, fluxes of them are considered to be asymptotic value. In this case, fluxes of resonance groups become a recursive algorithm which will be solved group by group.

For the next section of this paper, the theoretical model and derivation procedure of FSM will be clarified in Section 2 in detail. Section 3 illustrates the numerical validation of the FSM compared with traditional subgroup method and ultra-fine group method for both accuracy and efficiency. Section 4 will summarize the whole paper and give the main conclusion and discussion.

2. Theoretical model

2.1. Subgroup method

Subgroup method describes the severe change of resonance cross section by subgroup parameters, namely subgroup levels σ_i and subgroup weights ω_i, which correspond to the magnitude of cross section and the width of energy range of each subgroup respectively. In this condition, effective resonance cross section σ_x can be obtained by the following equation:

$$\sigma_{x,g} = \frac{\int_{\Delta E_i} dE \sigma_{x,i}(E)\varphi_i(E)}{\int_{\Delta E_i} dE \varphi_i(E)} = \frac{\sum_i^I \frac{\Delta E_i}{E_g}\sigma_{x,i}\varphi_i}{\sum_i^I \frac{\Delta E_i}{E_g}\varphi_i} = \frac{\sum_i^I \omega_i \sigma_{x,i}\varphi_i}{\sum_i^I \omega_i \varphi_i} \tag{1}$$

In Eq. (1), φ_i is the subgroup flux, which could be calculated by solving subgroup neutron transport equations. In the procedure of generating subgroup parameters, the fuel is supposed to be composed of one resonant nuclide R and hydrogen H. Based on the intermediate resonance approximation, the flux can be written as follows in the uniform condition:

$$\varphi_g = \frac{\lambda_R \Sigma_{p,R} + \lambda_H \Sigma_{p,H}}{\left(\Sigma_{a,R} + \lambda_R \Sigma_{s,R} + \lambda_H \Sigma_{p,H}\right)} = \frac{\sigma_b}{\left[\sigma_{a,R} + \lambda\left(\sigma_{s,R} - \sigma_{p,R}\right) + \sigma_b\right]} \tag{2}$$

In Eq. (2), λ is the intermediate resonance factor, Σ_a and σ_a are absorption cross sections, Σ_p and σ_p are potential scattering cross sections and σ_b is background cross section. The definition of background cross section can be shown as:

$$\sigma_b = \frac{\lambda_R \Sigma_{p,R} + \lambda_H \Sigma_{p,H}}{N_R} \tag{3}$$

In Eq. (3), N_R is the number density of resonant nuclide. Up till now, the unknown terms in Eq. (1) are only subgroup levels and subgroup weights. If the subgroup number is set as I there will be $2I$ unknown terms in total. Moreover, the normalization of subgroup weights can also be used as a constraint, which is shown in Eq. (4). Under this circumstance, there should be $2I-1$ set of background cross sections with corresponding effective resonance cross sections used to solve the unknowns. Through NJOY program or other continuous energy methods, resonance cross sections of different dilutions and temperatures can be generated for each resonance group and each nuclides respectively (Joo et al., 2009; Peng et al., 2013; Zhang et al., 2018d). Therefore, the subgroup parameters can be calculated in the following procedure (Jung et al., 2013; Li et al., 2018):

- Select $2I-1$ set of pre-generated resonance cross sections in different background cross sections, the $2I-1$ un-known quantities in Eq. (1) can be directly calculated by numerical analysis method. In this work, Pade approximation is adopted to solve the subgroup parameters (Hebert, 2009b).
- Repeat the above process until the subgroup parameters of all resonant nuclides are generated.

$$\sum_{i}^{I} \omega_i = 1 \tag{4}$$

Observed from Eq. (1), when all the subgroup parameters are generated, the subgroup flux in actual heterogeneous fuel area is still unclear. To solve this problem, the subgroup fixed source equation is deduced. In steady-state conditions, Boltzmann transport equation can be written as follows:

$$\begin{aligned}&\Omega \cdot \nabla \varphi(r,\Omega,E) + \Sigma_t(r,E)\varphi(r,\Omega,E)\\ &= Q_s(r,\Omega,E) + Q_f(r,\Omega,E) + S(r,\Omega,E)\end{aligned} \tag{5}$$

In Eq. (5), $\varphi(r,\Omega,E)$, $\Sigma_t(r,E)$, $Q_s(r,\Omega,E)$, $Q_f(r,\Omega,E)$ and $S(r,\Omega,E)$ are neutron flux, macro total cross section, scattering source, fission source, and external source respectively.

As the upper limit of resonance energy range is set to be 9118 eV, which is far less than the energy of most fission neutron, so the fission source is neglected in resonance calculation. Besides, the scattering source is assumed in the condition where only down-scattering reaction from high-energy groups to lower ones are taken into account. By introducing intermediate resonance factor, for subgroup i of resonance groupg, Eq. (5) can be simplified to a fixed source equation as below:

$$\begin{aligned}&\Omega \cdot \nabla \varphi_{g,i}(r,\Omega) + \Sigma_{t,g,i}(r)\varphi_{g,i}(r,\Omega)\\ &= \frac{1}{4\pi}\left[(1-\lambda_g)\Sigma_{s,g,i}\varphi_{g,i}(r) + \Sigma_{b,g}\right]\end{aligned} \tag{6}$$

In Eq. (6), λ_g is the intermediate resonance factor and $\Sigma_{b,g}$ is macro background cross section and its definition is shown in Eq. (7), in which M is the total number of nuclides types, N_m and $\Sigma_{p,g,m}$ are the number density and potential scattering cross section of nuclide m respectively. It can be observed that Eq. (6) has the same formation as the Boltzmann transport equation, so it can be solved by the same transport method and each group can be treated individually.

$$\Sigma_{b,g} = \sum_{m}^{M} \lambda_{m,g} N_m \Sigma_{p,g,m} \tag{7}$$

2.2. Ultra-fine group method

The basic idea of ultra-fine group method is to divide the resonance group into an exceedingly detailed energy mesh, then the slowing down equation is established and the ultra-fine fluxes are solved group by group. As is illustrated in Section 2.1, the fission source and up-scattering source is neglected for resonance groups, so that the neutron slowing down equation can be written as below:

$$\begin{aligned}&\Omega \cdot \nabla \varphi(r,u,\Omega) + \Sigma_t(r,u)\varphi(r,u,\Omega)\\ &= \sum_{n} \int_{u-\Delta_m}^{u} \Sigma_{m,s}(r,u)\varphi(r,u)\frac{e^{(u'-u)}}{1-\alpha_m}du'\end{aligned} \tag{8}$$

In Eq. (8), u is the lethargy, m represents for each nuclide and α_m is calculated by $(A_m-1)^2/(A_m+1)^2$, where A_m is the atom mass of nuclide m and $\Delta_m = 1 - \ln(\alpha_m)$. As the width of each ultra-fine group is much less than the largest lethargy obtained by a neutron from the collision with heavy nuclide, neutrons will be down-scattered into a large number of groups. Therefore, the source item of Eq. (8) can be shown as:

$$Q_g = \sum_{m}^{M}\sum_{n}^{N} P_{n,m}\Sigma_{s,g-n}\varphi_{g-n}\Delta u_f \tag{9}$$

In Eq. (9), $P_{n,m}$ is the probability of a neutron scattered over n ultra-fine groups after collision with nuclide m, N is the maximum number of ultra-fine groups covered by down-scattering and Δu_f is the ultra-fine group width. If we define $P(u'-u)$ as the probability of a neutron whose lethargy is decreased from u' to u after on collision, it can be calculated by Eq. (10).

$$P(u'-u) = \frac{1}{1-\alpha}e^{(u'-u)} \tag{10}$$

Therefore, the possibility for a neutron flying over n ultra-fine groups can be shown as:

$$\begin{aligned}P_n\Delta u_f &= \frac{1}{1-\alpha}\int_{u_0}^{u_0+\Delta u_f} du \int_{u_0-n\Delta u_f}^{u_0-(n-1)\Delta u_f} du' e^{(u'-u)}\\ &= \frac{1}{1-\alpha}\left(1-e^{-\Delta u_f}\right)^2 e^{-(n-1)\Delta u_f}\end{aligned} \tag{11}$$

From Eq. (10) and Eq. (11), it can be observed that $P_n = e^{-\Delta u_f}P_{n-1}$. Therefore, by combining Eq. (9) to Eq. (11), the recurrence relation among each scattering source of ultra-fine group can be deduced, which is shown in Eq. (12).

$$Q_g = Q_{g-1}e^{-\Delta u_f} + P_1\Sigma_{s,g-1}\varphi_{g-1} - P_L\Sigma_{s,g-L-1}\varphi_{g-L-1}e^{-\Delta u_f} \tag{12}$$

Observed from Eq. (12), the only unknown value is the flux of the first resonance group. However, the neutrons which are scattered into the first resonance group all come from the fast group, of which the fluxes are still unclear. Fortunately, variations of cross sections in fast group are flat enough to make the fluxes conform to 1/E law. In this case, the scattering source for the first resonance group can be easily calculated by asymptotic flux. Once the scattering source of the first resonance group is clear, flux of the first group can be obtained by solving a fixed source equation. Afterwards, the flux of the first group will be used to obtain the scattering source of the second group by Eq. (12), and the same procedure will be repeated for all the following groups until the flux of the last group is clear (Kim and Hong, 2011).

2.3. Fine-mesh subgroup method

The direct interpretation of fine-mesh subgroup method (FSM) is the coupling of the subgroup and ultra-fine method, which indicates that a fine mesh with subgroup parameters is established for resonance groups. However, problems of efficiency and geometry adaption will arise as the number of group increases, so that relevant optimizing methods are also applied to FSM. The following section will be divided into several parts. First, the selection of group structure and subgroup parameter generation procedure will be illustrated. The next part will focus on micro level optimization based on "one-group" approximation, which is aimed to diminish the number of subgroup fixed source equations. Finally, group condense scheme based on slowing down equation will be clarified.

2.3.1. Fine-mesh structure and subgroup parameters generation

Traditional resonance energy range is from 4 eV to 9118 eV, which is sufficient enough for typical uranium dioxide fuel. However, Plutonium isotopes such as Pu-242 also have prominent resonance peak near the upper thermal energy range, which would cause obvious errors for materials like MOX fuel if no treatment measure is carried out. In this work, resonance energy range is adapted as 1.855 eV to 9118 eV, which is the same as that of HELIOS-1.11 library. There are some existing researches on the finer mesh group structure, such as WLUP 172 groups (Leszczynski, 2002), SHEM 361 groups (Hfaiedh and Santamarina, 2005, 2008) or SHEM 295 groups (Canbakan and Hebert, 2015a, b). However, the existing structures do not consider the resonance

effect under 4 eV. Although SHEM structure has a fine mesh for resonance peak of U-238 around 6.7 eV, those from 22.5 eV to 100 eV are still not sufficiently described. Moreover, it is only the cross sections in resonance regions that are considered in FSM, data of fast groups are only used for the next step group condensation while data of thermal groups will not be used as up-scattering to resonance group is neglected.

Therefore, this work adopts a 408 group structure, of which the number of fast, resonance and thermal groups are 56, 289 and 63 respectively. Group structures of energy beyond 100 eV and below 1.855 eV are referenced from those of SHEM 361-groups structure. For energy range from 1.855 eV to 100 eV where resonance peaks mostly occur, a set of newly raised 217 group structure is developed and most groups are assigned around 2.8 eV, 6.7 eV, 20 eV, and 40 eV to capture the resonance peaks of U-238 and Pu isotopes. Subgroup parameters will be generated for 289 resonance groups according to theory introduced in Section 2.1 by the self-developed subgroup parameter calculating code (Li et al., 2018). Multi-group cross section and other smooth data needed in this procedure are provided by NJOY program. Since too large subgroup number can easily cause numerical instability and high calculation burden, we make it a rule that the largest number of subgroups is limited to be 5. Before the subgroup parameter generation, a series of resonance cross section table can be pre-made by NJOY program or other continuous energy programs. First, there is a trigger defined by Eq. (13), in which the Resonance Factor (*RF*) indicates for the variation degree of resonance cross section with the increase of background cross section. $\sigma_{t,\infty}$ is the total cross section in infinite-dilution condition and $\sigma_{t,10}$ is represents for conditions where background cross section is 10 bar. If $RF < 0.01$, it means that the resonance self-shielding effect is very small in this group, so that the effective cross section in this group can be just interpolated from the multi-group library. However, if $RF > 0.01$, subgroup parameter generation procedure will be carried out.

$$RF = \left| \frac{\sigma_{t,\infty}}{\sigma_{t,10}} - 1 \right| \tag{13}$$

There are two criteria adopted to check the adaptability of subgroup parameters calculated. First, the subgroup levels used in subgroup fixed source equations must be positive values. The next is the relative error (*RE*) defined by Eq. (14) of re-produced cross section table by subgroup parameters should be no more that 1%. In the calculating process, since we cannot pre-decide which value is the best choice, the subgroup number will be chosen from 2 to 5 gradually until the criteria above are meet.

$$RE = \frac{\left| \frac{\sum_i^l \omega_i \sigma_{x,i} \frac{\sigma_b}{\left[\sigma_{a,i}+\lambda\left(\sigma_{s,i}-\sigma_{p,i}\right)+\sigma_b\right]}}{\sum_i^l \omega_i \frac{\sigma_b}{\left[\sigma_{a,i}+\lambda\left(\sigma_{s,i}-\sigma_{p,i}\right)+\sigma_b\right]}} - \sigma_x(\sigma_b) \right|}{\sigma_x(\sigma_b)} \times 100\% \tag{14}$$

As the Pade approximation used in this work is a pure mathematical process, numerical instability may occur and subgroup parameters generated could have impractical values like negative cross sections, which will result in the inability to solve subgroup fluxes. To avoid this situation, two measures are adopted. First, according to Section 2.1, the maximum number of different diluted cross sections used by Pade approximation is 9 as the largest subgroup number is 5. To provide more diversified choices, a set of cross section in over 30 diluted conditions from 10 bar to 10^{10} bar are pre-generated in this work. A traversing procedure is added to the subgroup parameter generating code to find the best set of $2N - 1$ diluted cross sections. If none of the existing choices satisfy the numerical stability and accuracy requirement, *RE* requirement would be added by 0.1%, then the above procedure will be repeated until all subgroup parameters are generated.

2.3.2. One-group micro level optimization

Traditional subgroup method solves subgroup fixed source equations for each subgroup and each nuclide respectively. For structures like WLUP 69 or HELIOS 47 groups, subgroup fixed source problems do not account for the vast majority of the whole calculating procedure as there are no more than 20 resonance groups in total. However, 289 resonance groups of FSM leads to a sharp rise in calculating burden. Table 1 shows the sum of subgroup number of all 289 resonance groups for some typical resonant nuclides in a MOX fuel. It can be seen that up to 4221 subgroup fixed source equations are needed to be solved in a flat source region, which is obviously unacceptable for lattice scale problems.

There are two main points to reduce the number of subgroup fixed equations. On the one hand, although the number of resonance groups increases greatly for FSM, group dependent smooth data like $\lambda\sigma_p$ of the main moderating nuclide, such as hydrogen, almost remain the same for all resonance groups. Therefore, the number of neutrons scattering into each resonance groups do not change severely regardless of the group structure. It provides the feasibility to get a group-averaged source item for all subgroup fixed source equations of a certain resonant nuclide. On the other hand, several studies have proved that escape cross sections obtained by subgroup fluxes can be interpolated (Stamm'ler, 2008; Jung et al., 2013; Park and Joo, 2018) by both micro or macro levels of subgroups. Combing these two theories together, we propose the one-group micro level optimization method, which solves subgroup fixed source equations for each resonant nuclide with a pre-selected subgroup levels just for one resonance group. In this method, "one-group" indicates that all the resonance groups are treated as a whole since they are assigned with the same set of subgroup levels and smooth data for fixed source equations. The group-averaged smooth data is expressed as Eq. (15).

$$\sigma_x = \frac{\sum_g^G \sigma_{xg} RI_{g,\infty} \Delta u_g}{\sum_g^G RI_{g,\infty} \Delta u_g} \tag{15}$$

In Eq. (15), G is the number of resonance groups. For resonant nuclide, $RI_{g,\infty}$ represents its absorption resonance integral of group g. For non-resonant nuclide, $RI_{g,\infty}$ adopts the value of the current resonant nuclides in process.

$$\Omega \cdot \nabla \varphi_i(r,\Omega) + \left(N_r \sigma_{t',i} + \sum_m^M \lambda_m \Sigma_{p,m} \right) \varphi_i(r,\Omega) = \frac{1}{4\pi} \sum_m^M \lambda_{m,g} \Sigma_{p,m} \tag{16}$$

For one-group subgroup fixed source equations of resonant nuclide r, Eq. (6) can be transformed into the form showed in Eq. (16), where $\sigma_{t',i} = \sigma_{t,i} - (1-\lambda)\sigma_{s,i}$. Observed from Eq. (16), $\sum_m^M \lambda_{m,g} \Sigma_{p,m}$ represents for the background conditions for the whole material. However, micro levels of $\sigma_{t',i}$ are unclear for one-group approximation as we do not have group-average subgroup parameters. Moreover, it can be noticed that subgroup weights are not used in this procedure, so we only need to determine a set of micro levels of $\sigma_{t',i}$. This procedure is shown as follows.

$$\sigma_e = \frac{\sigma_{t',i} \varphi_i}{1 - \varphi_i} - \sum_m^M \lambda_m \sigma_{p,m} \tag{17}$$

Escape cross section of group g can be calculated by Eq. (17), so we can get the corresponding relations between σ_e and $\sigma_{t',i}$ at different rings of fuel cell, which is shown in Fig. 1, where the total number of rings in the fuel pin is chosen as 5. It can be seen that the pin averaged σ_e does not change much with the increase of

Table 1
Total subgroup number of all resonance groups.

Nuclide	U-235	U-238	Pu-238	Pu-239	Pu-240	Pu-241	Pu-242	Am-241
Total subgroup number	611	475	470	540	457	553	430	685

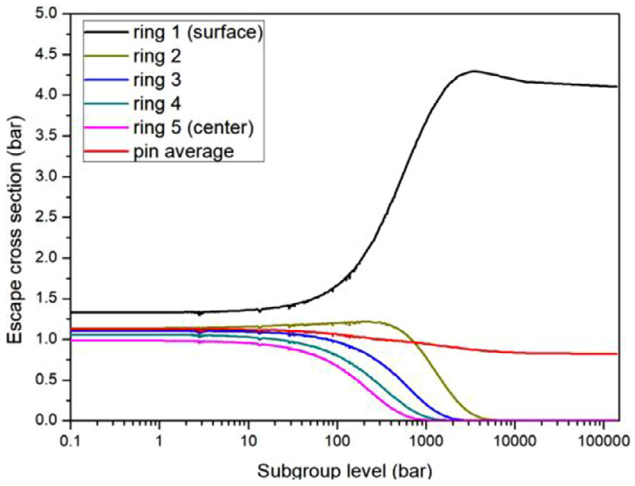

Fig. 1. Variation of escape cross section by subgroup level.

subgroup level, but it shows an obvious variation for different rings, especially for the outermost ring. However, σ_e for subgroup levels under 10 bar or above 10^4 bar for each ring and the whole pin have little change, so σ_e in these levels could just adopts that value of 10 and 10^4 bar respectively since it almost remains the same. For levels between 10 and 10^4 bar, more attention should be paid and the number of levels should be added. A series of sensitivity test for different choices of micro levels are carried out to determine the final selection. In this test, the number of levels between 10 and 10^4 bar is increased from 2 to 10 gradually for calculations of different pin cells to find the optimized setting. The detailed numerical process will not be illustrated in this paper since it is too lengthy and tedious. The final selection of number is 6 and these values is set to be 100, 200, 300, 500, 1000 and 2000 bar.

However, the pre-determined subgroup levels will not always be the same as actual subgroup levels, which are calculated numerically with subgroup weights together in each resonance group respectively. To get the subgroup fluxes for each resonance group from those of "one-group", an interpolation process is carried out. To avoid numerical problems, it is σ_e defined in Eq. (17) rather than φ_i that used in interpolation. The dependence between σ_e and $\sigma_{t',i}$ is established, and the new σ_e will be obtained by liner interpolation by $ln\left(\sigma_{t',i}\right)$ (Stamm'ler, 2008).

2.3.3. Group condense scheme for FSM

To capture the spectrum shape of the flux of resonance groups, recursive slowing down equations used in ultra-fine group method are also adapted in FSM. However, different from ultra-fine group method, lethargies of resonance groups for FSM are not always less than those of neutron collision. As the group number of FSM is several orders of magnitude smaller than that of ultra-fine group, so the scattering cross sections in source item of slowing down equation can just be provided by the exact scattering matrix, which can be generated by NJOY program. Similarly, the fission source and up-scattering effect in resonance region are not taken into consideration. In this case, for group g, Eq. (8) can be transformed in Eq. (18):

$$\Omega \cdot \nabla \varphi_g + \sum_m^M \Sigma_{m,t,g} \varphi_g = \sum_m^M \sum_{g'}^{g-1} \Sigma_{m,s,g' \to g} \varphi_{g'} \tag{18}$$

In Eq. (18), $\Sigma_{m,t,g}$ is the total cross section of group g for nuclide m, $\Sigma_{m,s,g' \to g}$ is the scattering cross section from group g' to g and $\varphi_{g'}$ is the flux of upper group g'. Once the fluxes of the upper resonance groups are determined, Eq. (18) is transformed into a fixed source equation, which will be easy for the transport module to solve. Just like ultra-fine group method, we also adopt the asymptotic flux to calculate the scattering source from the fast group in FSM, then the flux of the first resonance group could also be produced by solving fixed source equation. Subsequently, fluxes of the following resonance groups will be solved group-by-group by analogy. The final effective resonance cross section for σ_x can be obtained by conservation of reaction rate, which is shown in Eq. (19).

$$\sigma_x = \frac{\sum_g^G \sigma_{x,g} \varphi_g}{\sum_g^G \varphi_g} \tag{19}$$

3. Numerical validation

The resonance group number for FSM is set as 289 and its energy range is from 1.8554 to 9118 eV. The condensed group structure is adopted from HELIOS-47 library, of which the resonance energy range is the same with FSM while the resonance group number is 16. The method proposed above is applied to a series of benchmark consisted of single pin cell problems and lattice problems. The reference resonance cross sections and effective multiplication factors are provided by the Monte Carlo method. To compare the calculating results with traditional methods, the self-developed codes by subgroup method (SGM) with Bondarenko iteration method (Li et al., 2019) and ultra-fine group method (UFG) combined with MOC are adopted in this paper. FSM, SGM, and UFG are all based on the same ENDF/B VII.0 library version and the same transport module based on method of characteristics (Song et al., 2019) is applied to both fixed source problems and eigenvalue problems. Group structure of SGM is HELIOS-47 group and the subgroup parameters are set for 16 resonance groups. UFG has 34,000 resonance groups and the fluxes are calculated by solving slowing-down equations. Resonance group number of FSM and UFG will both condensed to the same as SGM. Resonance cross sections and effective multiplying factors calculated by these methods will be compared and analyzed in this section.

3.1. Single cell problems

Two single cell problems are employed in this work for testing the resonance calculating capability for FSM. The first one is a typical PWR UO_2 fuel pin with 6.5 wt% U-235 in cold state and the next is a UO_2 pellet in high burn-up conditions with the average burnup is 74.5 GWd/t. These two problems have the same geometrical configuration and dimensions. To capture the resonance interference in detail as well as space self-shielding caused by rim effect, the fuel pin is divided into 3 and 17 rings respectively for these two problems, which are shown in Fig. 2. The outer-most ring for both pellets is clad consisted of natural zircalloy while

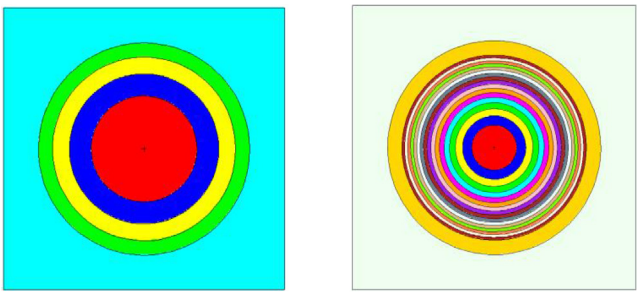

(a) UO_2 (b) High burn-up UO_2

Fig. 2. Geometry configuration of UO_2 and high burn-up UO_2 pellet.

the inner rings of fuel rod are divided by the same volume. However, the UO_2 pin shares the same material composition in the whole fuel are while the nuclide densities of the burn-up UO_2 case has an obvious spatial distribution along the radial direction. The detailed nuclide density and geometry dimensioning value are referenced from benchmarks (Yamamoto et al., 2002) and (Matsumoto et al., 2005) respectively. The reference values are calculated by MCNP5 program (X-5 Monte Carlo Team, 2003), in which the total particle number is 100,000 and 300 generations excluded the first 50 are counted into the reference results for both pellets. The calculations for FSM, SGM and UFG are performed with double precision with the following MOC parameters: 3 polar angles and 16 azimuthal angles per octant, 0.01 cm ray spacing Tabuchi-Yamamoto quadrature (Yamamoto et al., 2007) for UO_2 while 0.001 cm for burn-up burn-up UO_2.

3.1.1. Typical UO_2 pellet

For UO_2 pellet, the relative error of pin-average absorption cross section of U-238 and U-235 as well as neutron production of U-235 are shown in Figs. 3 and 4 respectively. It can be seen that FSM and UFG have a good performance in general for both two resonant nuclides while SGM has a large deviation, especially for U-235. As UFG has 34,000 groups in resonance region, it is detailed enough to describe the self-shielding effect. By contrast, it can be seen that FSM has similar precision as UFG but with only 289 groups because subgroups also offer further discretion. For resolvable resonance region, especially for energies below 100 eV where resonance peaks always occur, results of FSM have a good agreement with the reference value. The maximum error of FSM for U-238 and

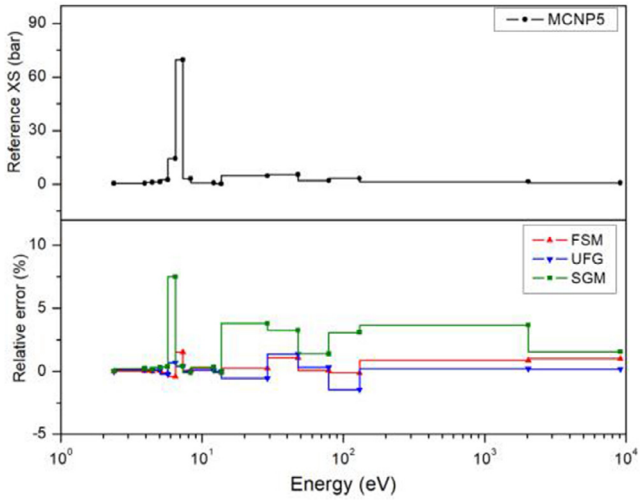

Fig. 3. Relative error of absorption cross section of U-238.

U-235 both occur in energy regions near the fast group since group number in this range is not as sufficient as that near the resonance peaks. However, the maximum error is still less than 1.5%, which is acceptable. SGM cannot deal with resonance interference effect accurately, which is mainly caused from influences of resonance peaks for U-238 to other resonant nuclides, so the accuracy of U-235 is unsatisfactory with the maximum error greater than −30%. Table 1 gives the calculating cost and eigenvalue errors of these three methods. The computer version used in this paper is i7-4510U 2.0 GHz. The number of fixed source equations is calculated by Eq. (20), where N_{fix} is the total fixed source equation number, N_{fsr} is the number of flat source regions, N_{res} is the number of resonant nuclides, N_{sub} is the number of subgroup levels, G_1 and G_2 is the number of resonance group number. N_{fsr} and N_{res} are the same value for all three methods. For FSM, $G_1 = 1,\ G_2 = 289$. For SGM, $G_1 = 16,\ G_2 = 0$. For SGM, $G_1 = 0,\ G_2 = 34,000$.

$$N_{fix} = N_{fsr}\left(N_{res}\sum_{g}^{G_1} N_{sub} + G_2\right) \tag{20}$$

Observed from Table 2, UFG has the most accurate result with only 18 pcm different from MCNP. However, as up to 34,000 fixed source equations are needed to be solved in each region, the calculating time is not acceptable and 1399.5 s have cost even for the simplest pellet. SGM has the highest efficiency as the total subgroup fixed source equations is only 51 and 55 for U-238 and U-235 respectively in each region, but it cannot provide the precise effective cross sections and error of eigenvalue is −551 pcm. By contrast, FSM has a relatively high accuracy for eigenvalue as 46 pcm is obtained. Moreover, number of fixed source equations for FSM is reduced by more than 99% compared with UFG while the accuracy remains at the same level. Although FSM spent about 80% more time than SGM, it is worthwhile as the total time is still acceptable for personal computers with 34.5 s.

3.1.2. Burn-up UO_2 pellet

Due to the rim effect, resonant nuclides will accumulate around the surface of fuel rod, number densities and reaction rate of resonant nuclides will also show great variations along the radial direction. Therefore, sub-pin calculating ability for rim effect and space self-shielding is particularly essential for resonance treatment in burn-up case. To capture this phenomenon, resonance cross sections in sub-pin scale, especially the variations along the radial direction are analyzed in this problem. As there are obvious resonance peaks for U-238 and Pu isotopes in energy regions between 6.476 eV–7.338 eV and 13.71 eV–29.02 eV, the spatial distribution of absorption cross sections of U-238, Pu-239 and Pu-240 in this energy range are shown respectively in Figs. 5–7.

Observed from Fig. 5, FSM can handle the radial distribution of resonance cross section of U-238 in burn-up condition accurately in general. For U-238, it can be seen that cross sections of both energy regions show an obvious increase from the center of the pin to the surface, this phenomenon results from the space self-shielding effect as the majority of neutrons are absorbed in the surface area, and both fluxes and reaction rate in the inner side will decrease sharply. Both FSM and UFG could give precise results as the maximum error of them are less than 2%. The maximum errors occur near the surface area as the fluxes near this regions have a severe deceasing trend. Moreover, although FSM has an underestimation while UFG has an overestimation of effect cross sections, the errors are both acceptable for reactor physics calculation. By contrast, SGM could not reproduce the accurate results, of which the largest error are more than 6% for both energy regions.

As for Pu isotopes, FSM has a better performance than U-238 that most of the errors are less than 1%. Pu isotopes are generated gradually during the burn-up process, and they will be accumu-

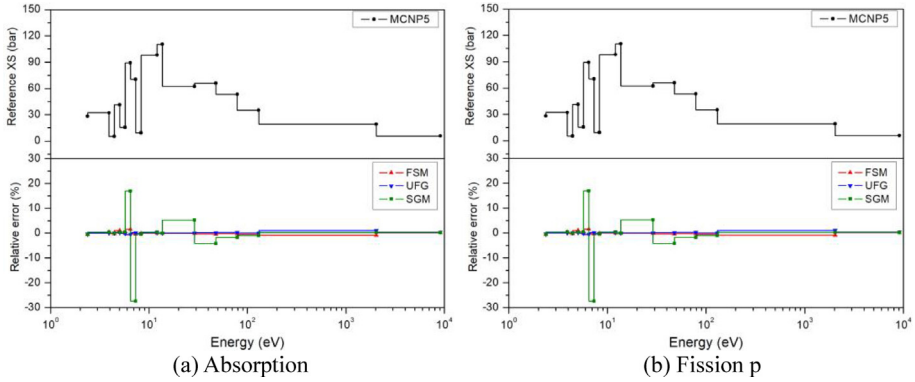

Fig. 4. Relative error of absorption cross section and fission production of U-235.

Table 2
Calculating cost and eigenvalue error of UO_2 pellet.

Method	Fixed source equation number	Time (s)	k_{eff} (pcm)	
MCNP	–	–	1.53226	–
FSM	1830	34.5	1.53272	46
UFG	204,000	1399.5	1.53208	−18
SGM	636	19.2	1.52675	−551

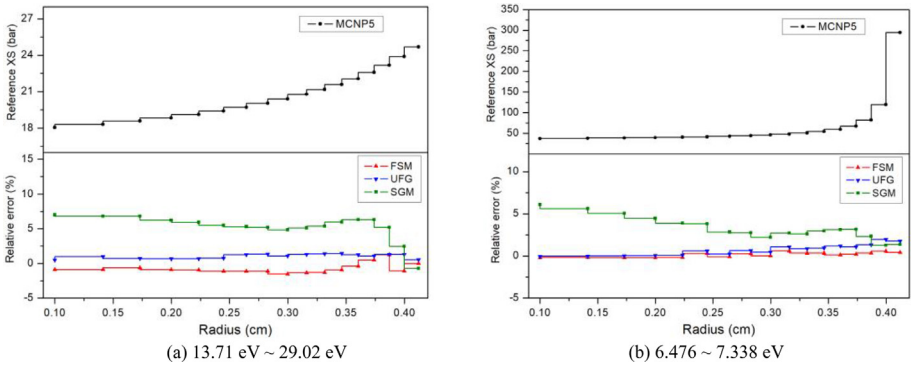

Fig. 5. Radial distribution of relative error of absorption cross section of U-238.

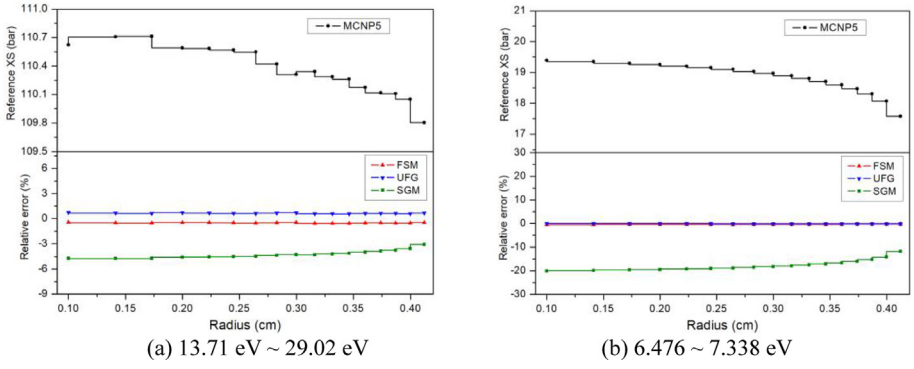

Fig. 6. Radial distribution of relative error of absorption cross section of Pu-239.

lated mainly near the surface due to the rim effect, so the self-shielding effect in this area is very difficult to handle. From Figs. 6 and 7, it can be seen that FSM can describe the rim effect as accurate as UFG, while SGM shows a large overestimation for U-238 and Pu-240 and an obvious underestimation for Pu-239. Table 3 displays the calculating cost and eigenvalue results of this problem. It can be seen that FSM has an improvement of over 88.5% for calculating speed compared with UFG with a similar level of accuracy, while 566 pcm less eigenvalue error with 24% more time than SGM. In addition, as the one-group micro level is adopted in FSM, the total number of subgroup fixed source equations is even less than that of SGM. With the number of resonant nuclides increase, fixed source equations of SGM will have a great increase since traditional subgroup method needs to treat each subgroup of

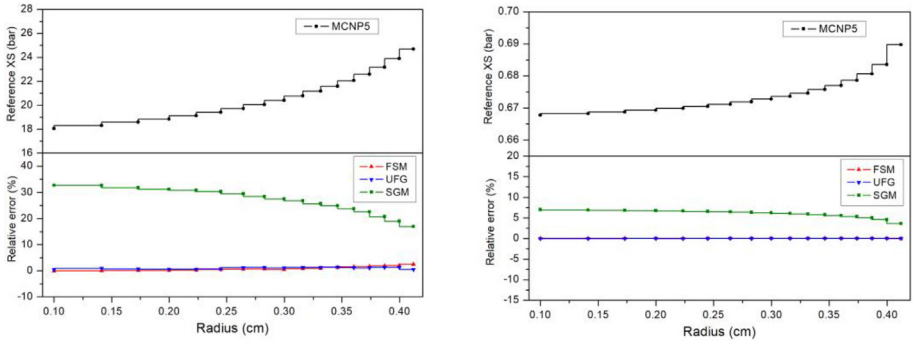

(a) 13.71 eV ~ 29.02 eV (b) 6.476 ~ 7.338 eV

Fig. 7. Radial distribution of relative error of absorption cross section of Pu-240.

Table 3
Calculating cost and eigenvalue error of burn-up UO_2 pellet.

Method	Fixed source equation number	Time (s)	k_{eff} (pcm)	
MCNP	–	–	1.18932	–
FSM	6900	835.1	1.18914	18
UFG	5,440,000	7269.2	1.18868	−64
SGM	6920	634.4	1.18347	−584

each resonance nuclides respectively. FSM only need 8 micro levels for each nuclide in each region, so that it is the slowing down calculation for group condensation accounts for the major part of fixed source equations. As there is interpolation process existing in FSM, its time consuming is still more than SGM, which is worth the price considering the accuracy.

3.2. Lattice problems

In this section, resonance calculation in lattice scale problems is tested. However, as the typical pellets have been already analyzed in Section 3.1, we select two severe conditions for lattice calculation which are shown in Fig. 8. The first one is a 3-by-3 lattice with UO_2 and MOX pin distributed crossly, and the other one is a BWR lattice with two Gadolinium pellets. The reference values are calculated by MCNP5 program, in which the total particle number is 200,000, and 300 generations excluded the first 50 are counted into the reference results for both pellets.

3.2.1. UO_2-MOX lattice

Adjacent fuel pins would influence the resonance interference calculation considerably. To test this problem, we have designed a 3-by-3 lattice consisted of MOX and UO_2 fuel pins. The geometry parameters of each pin cell is the same as the single cell problems in Section 3.1. The MOC parameters of this problem are 3 polar angles and 16 azimuthal angles per octant and 0.03 cm ray spacing Tabuchi-Yamamoto quadrature. The clad of all fuel rods is consisted of natural zircalloy and the moderator is light water. The lattice is in the cold state and the temperature is set to be 300 K in the whole region. For the UO_2 fuel, the U-235 enrichment is 6.5 wt%, while the Pu fissile content is 11 wt% for the MOX fuel (Yamamoto et al., 2002). Fig. 9 gives the relative error of pin-averaged absorption cross section of U-238 and Pu-239 in No. 3 MOX and Fig. 10 for U-238 and U-235 in No. 1 UO_2 pin.

We can see that most errors are less than 1% and the largest errors for all nuclides shown below are less than 2% for FSM. U-238 errors in MOX pin are relatively larger as resonance interference effect is severer. It can be observed that the errors of U-238, U-235 and Pu-239 do not show obvious increase compared with single cell problems above. In general, FSM has a good performance for UO_2 and MOX pin distributed crossly with the accuracy in the same level as that of infinite fuel pin. Table 4 gives the calculating cost and eigenvalue error of UO_2-MOX lattice, FSM has an error of 82 pcm.

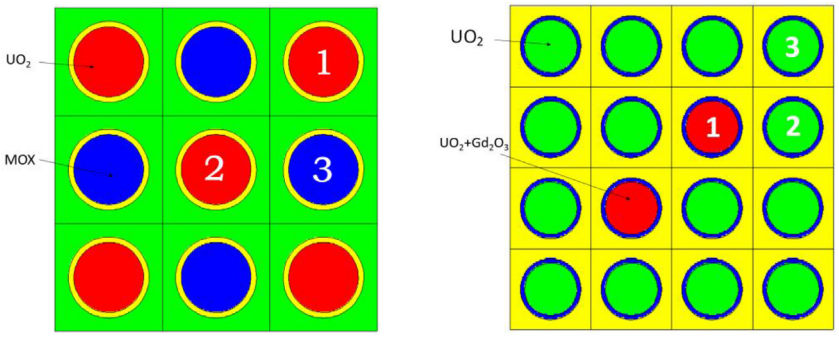

(a) UO_2-MOX lattice (b) BWR lattice

Fig. 8. UO_2-MOX lattice and BWR lattice with Gadoliniums.

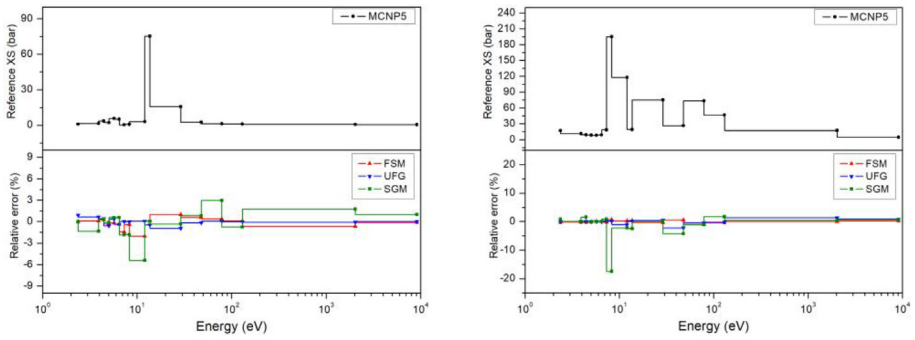

(a) U-238 (b) Pu-239

Fig. 9. Relative error of absorption cross section of U-238 and Pu-239 in No.3 MOX pin.

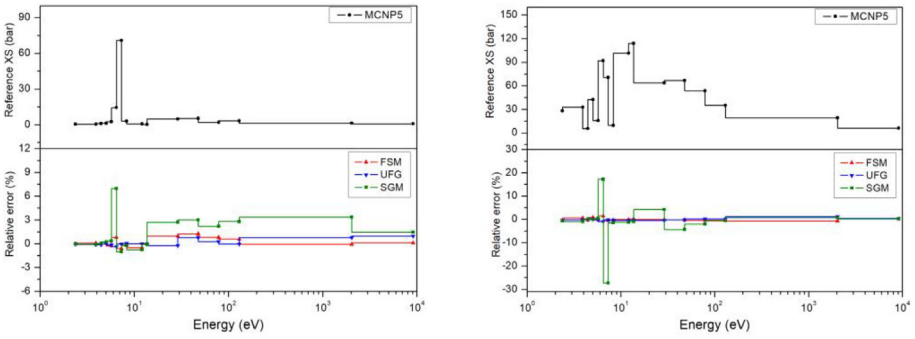

(a) U-238 (b) U-235

Fig. 10. Relative error of absorption cross section of U-238 and U-235 in No.1 UO_2 pin.

Table 4
Calculating cost and eigenvalue error of UO_2 – MOX lattice.

Method	Fixed source equation number	Time (s)	k_{eff} (pcm)	
MCNP		–	1.35551	–
FSM	155,088	911.5	1.35633	82
UFG	14,688,000	2357.2	1.35588	37
SGM	149,472	682.3	1.35053	−498

3.2.2. BWR lattice with Gadoliniums

For the second lattice, the fuel pin of UO_2 is divided by 3 rings while the gadolinium pin is divided by 10 rings to describe the sharp change of flux in the radial direction caused by the existence of strong absorbers. The MOC parameters of this problem are 3 polar angles and 16 azimuthal angles per octant and 0.01 cm ray spacing Tabuchi-Yamamoto quadrature. Detailed nuclide composition and geometry configuration is referenced from (Yang and Satvat, 2012). The calculating results of U-238, U-235, Gd-155 and Gd-156 in the No.1 Gadolinium rod are shown in Figs. 11 and 12 respectively.

For U-238 and U-235, the maximum errors of them in Gadolinium pin have a little rise for both FSM and UFG compared with UO_2 and MOX pin cell, which are both up to 2.5% for some energy ranges. However, most of the errors are still less than 1%, which is acceptable. As Gadolinium isotopes have a strong character for neutron absorption, it is difficult to predict the flux variations, so that the errors in this condition may increase. Observed from Fig. 12, Gd-155 has significant resonance peaks in energy under 10 eV, and there is also an obvious fluctuation of cross section between 10 and 100 eV. Errors for Gd-155 in these energy ranges are larger than others. As for Gd-156, two dominant resonance peaks occur in 29 to 47 eV and 79 to 130 eV and the largest error also lies here. Cross sections in other energy range are far smaller than the peak value and just seems to be flat with energy change. Gd-157 also has significant resonance peaks which occur around 4 eV, 30 eV and 79 to 130 eV. FSM and UFG could handle resonance effect of Gadolinium isotopes well even in the area where different resonance peaks overlap with each other, while SGM shows large deviations compared with reference value. Table 5 gives the calculating cost and eigenvalue calculating results and the error of FSM is 151 pcm. In general, although FSM shows an increase of error to deal with Gadolinium problem, the results of cross section and eigenvalue is still similar to that of UFG while decreasing the calculating burden greatly.

4. Conclusions and discussions

In order to handle the resonance self-shielding effect in complicated conditions, the fine-mesh subgroup method (FSM) is proposed in this work. FSM combines the subgroup method and ultra-fine group method together and a 289 resonance group structure is adopted. The concept of subgroup is used for further group discretization and group-by-group slowing-down equations are solved by method of characteristics for group condensation. To enhance calculating efficiency, the one-group micro level opti-

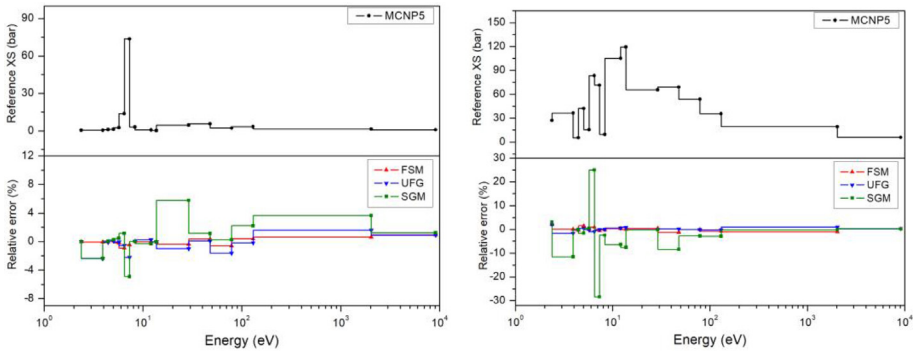

(a) U-238 (b) U-235

Fig. 11. Relative error of absorption cross section of U-238 and U-235 in No.1 Gd pin.

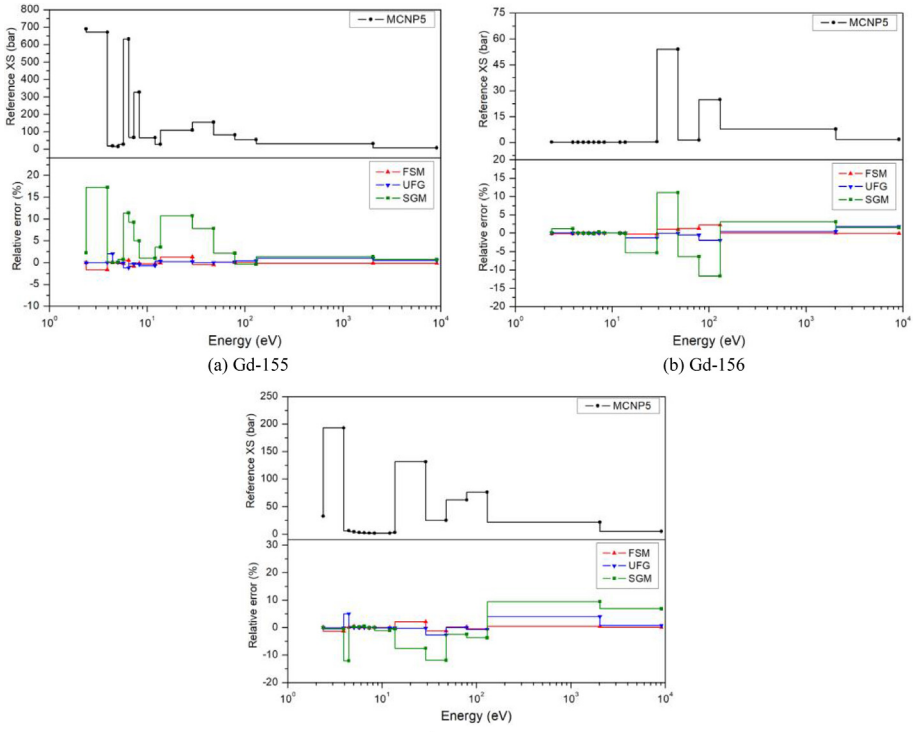

(a) Gd-155 (b) Gd-156

(c) Gd-157

Fig. 12. Relative error of absorption cross section of Gd-155, Gd-156, and Gd-157 in No.1 Gd pin.

Table 5
Calculating cost and eigenvalue error of BWR lattice with Gadoliniums.

Method	Fixed source equation number	Time (s)	k_{eff} (pcm)	
MCNP	–	–	1.22763	–
FSM	282,406	596.4	1.22914	151
UFG	284,920,000	9927	1.22867	104
SGM	241,344	382.3	1.22411	−402

mization method is proposed in this work. Each resonance nuclide only needs to solve subgroup fixed source equations for 8 times in each region and an interpolation process between escape cross sections are applied. FSM does not need extra resonance interference correction as the double discretization of resonance groups by fine mesh and subgroup is sufficient enough to describe the severe fluctuation of resonance cross sections. Numerical results show that for typical or complicated problems, FSM has the same accuracy level as the direct ultra-fine group method which needs 34,000 groups for resonance energy range and the calculating time is reduced by more than 80%.

However, although FSM has a great improvement in efficiency compared with ultra-fine group method, it still causes more consumption of time and memory than traditional subgroup method. According to the numerical analysis above, the advantages of FSM could be used in severer local resonance effect such as burn-up problems or cases with strong absorbers. For large scale typical problems and three-dimensional whole core calculation, more

improvement and verification work are under investigation and will be illustrated in the future work.

Declaration of Competing Interest

The authors declare that there is no conflict of interest.

Acknowledgments

This work is supported by the Science and Technology on Reactor System Design Technology Laboratory, Heilongjiang Province Science Foundation for Youths [QC2018003], Nuclear Power Technology Innovation Center, Fundamental Research Funds for the Central Universities [grant number GK2150260178], and the Research on Key Technology of Numerical Reactor Engineering [J121217001].

Appendix A. Supplementary data

Supplementary data to this article can be found online at https://doi.org/10.1016/j.anucene.2019.106992.

References

Askew, J., Fayers, F., Kemshell, P., 1966. A general description of lattice code WIMS. J. Br. Nucl. Energy Soc. 5, 546–585.
Cacuci, D., 2010. Handbook of Nuclear Engineering. Springer, pp. 1035–1047.
Canbakan, A., Hebert, A., 2015a. Accuracy of s subgroup method for pressurized water reactor fuel assembly models. International Conference on Mathematics and Computation.
Canbakan, A., Hebert, A., 2015b. Accuracy of a 2-level scheme based on a subgroup method for pressurized water reactor fuel assembly models. Ann. Nucl. Energy 81, 164–173.
Chen, J., Liu, Z., Zhao, C., He, Q., Zu, T., Cao, L., Wu, H., 2018. A new high-fidelity neutronics code NECP-X. Ann. Nucl. Energy 116, 417–428.
Choi, S., Lee, C., Lee, D., 2017. Resonance treatment using pin-based pointwise energy slowing-down method. J. Comput. Phys. 330, 134–155.
Cullen, D., 1977. Calculation of Probability Table Parameters to Include Intermediate Resonance Self-Shielding. Lawrence Livermore National Laboratory. UCRL-79761.
Downar, T., Kochunas, B., Collins, B., 2016. Validation and verification of the MPACT code. PHYSOR 2016.
Hebert, A., Marleau, G., 1991. Generalization of the stamm'ler method for the self-shielding of resonant isotopes in arbitrary geometries. Nucl. Sci. Eng. 108 (3), 230–239.
Hebert, A., Santamarina, A., 2008. Refinement of the Santamarina-Hfaiedh energy mesh between 22.5 eV and 11.4 keV. International Conference on Reactor Physics.
Hebert, A., 2009a. Development of the subgroup projection method for resonance self-shielding calculations. Nucl. Sci. Eng. 162, 56–75.
Hebert, A., 2009b. Applied Reactor Physics. Presses Internationales Polytechnique, pp. 225–228.
Hfaiedh, N., Santamarina, A., 2005. Determination of the optimized SHEM mesh for neutron transport calculations. International Conference on Mathematics and Computation.
Ishiguro, Y., Takano, H., 1971. PEACO: A Code for Calculation of Group Constant of Resonance Energy Region in Heterogeneous Systems. Japan Atomic Energy Research Institute. No.JAERI-1.
Joo, H.G., Cho, J.Y., Kim, K.S., Lee, C.C., Zee, S.Q., 2004. Methods and performance of a three-dimensional whole-core transport code DeCART. PHYSOR 2004.
Joo, H.G., Kim, G.Y., Pogosbekyan, L., 2009. Subgroup weight generation based on shielded pin-cell cross section conservation. Ann. Nucl. Energy 36 (7), 859–868.
Jung, Y.S., Shim, C.B., Lim, C.H., Joo, H.G., 2013. Practical numerical reactor employing direct whole core neutron transport and subchannel thermal/hydraulic solvers. Ann. Nucl. Energy 62, 357–374.
Kim, K.S., Hong, S.G., 2011. The method of characteristics applied to solving slowing down equation to estimate the self-shielded resonance cross sections with an explicit geometrical effect. Ann. Nucl. Energy 38 (2–3), 438–446.
Kim, K.S., Williams, M.L., Wiarda, D., Andrew, T., 2015. Development of a new 47-consortium for advanced group simulation library of for the CASL neutronics simulator. International Conference on Mathematics and Computation.
Kochunas, B., Collins, B., Jabaay, D., Downar, T.J., Martin, W.R., 2013. Overview of development and design of MPACT: Michigan Parallel Characteristics Transport Code. International Conference on Mathematics and Computation.
Leszczynski, F., 2002. Description of WIMS library update project (WLUP). International Meeting on Reduced Enrichment for Research and Test Reactors.
Li, S., Zhang, Q., Zhao, Q., Li, P., 2018. Calculation method for subgroup parameters with accurate resonance interference treatment. At. Energy Sci. Technol. 52 (7), 1166–1173.
Li, S., Zhang, Z., Zhang, Q., Hao, C., Zhao, Q., 2019. Analysis of categorical subgroup method for resonance self-shielding treatment. Front. Energy Res. 7 (48), 1–12.
Liu, Z., He, Q., Zu, T., Cao, L., Wu, H., Zhang, Q., 2018. The pseudo-resonant-nuclide subgroup method based global–local self-shielding calculation scheme. J. Nucl. Sci. Technol. 55 (2), 217–228.
Liu, Y., Martin, W., Williams, M., Kim, K., 2015. A full-core resonance self-shielding method using a continuous-energy quasi-one-dimensional slowing-down solution that accounts for temperature-dependent fuel subregions and resonance interference. Nucl. Sci. Eng. 180, 247–272.
Macfarlane, R., Muir, D.W., Boicourt, R.M., Kahler III, A.C., Conlin, J.L., 2016. The NJOY Nuclear Data Processing System, Version 2016. Los Alamos National Laboratory. LA-UR-17-2..
Matsumoto, H., Ouisloumen, M., Takeda, T., 2005. Development of spatially dependent resonance shielding method. J. Nucl. Sci. Technol. 42 (8), 688–694.
Nikolaev, M., Ignatov, A., Isaev, N., Khokhlov, V., 1971. The method of subgroups for considering the resonance structure of the cross sections in neutron calculations. Sov. At. Energy 30, 426–430.
Park, H.J., Kim, K.S., Hong, S.G., Song, J.S., 2017. An improved DeCART library generation procedure with explicit resonance interference using continuous energy Monte Carlo calculation. Ann. Nucl. Energy 105, 95–105.
Park, H., Joo, H.G., 2018. Effective subgroup method employing macro level grid optimization. PHYSOR 2018.
Peng, S., Jiang, X., Zhang, S., Wang, D., 2013. Subgroup method with resonance interference factor table. Ann. Nucl. Energy 59, 176–187.
Powney, D.J., Newton, T.D., 2004. Overview of the WIMS 9 Resonance Treatment. SERCO, ANSWERS/WIMS/TR 26 (1).
Rhodes, J., Smith, K., Lee, D., 2006. CASMO-5 development and applications. PHYSOR 2006.
Song, P., Zhang, Z., Liang, L., Zhang, Q., Zhao, Q., 2019. Implementation and performance analysis of the massively parallel method of characteristics based on GPU. Ann. Nucl. Energy 131, 257–272.
Stamm'ler, 2008. HELIOS Methods. Studsvik Scandpower.
Sugimura, N., Yamamoto, A., 2007. Resonance treatment based on ultra-fine-group spectrum calculation in the AEGIS code. J. Nucl. Sci. Technol. 44 (7), 958–966.
Williams, M.L., 1983. Correction of multigroup cross sections for resolved resonance interference in mixed absorbers. Nucl. Sci. Eng. 83, 37–49.
X-5 Monte Carlo Team, 2003. MCNP – A General N-Particle Transport Code, Version 5 – Volume I: Overview and Theory LA-UR-03-1987. Los Alamos National Laboratory.
Yamamoto, A., Ikehara, T., Ito, T., Saji, E., 2002. Benchmark problem suite for reactor physics study of LWR next generation fuels. J. Nucl. Sci. Technol. 39 (8), 900–912.
Yamamoto, A., Tabuchi, M., Sugimura, N., Ushio, T., Mori, M., 2007. Derivation of optimum polar angle quadrature set for the method of characteristics based on approximation error for the Bickley function. J. Nucl. Sci. Technol. 44 (2), 129–136.
Yang, X., Satvat, N., 2012. Annals of Nuclear Energy MOCUM: a two-dimensional method of characteristics code based on constructive solid geometry and unstructured meshing for general geometries. Ann. Nucl. Energy 46, 20–28.
Zhang, Q., Wu, H., Cao, L., Zheng, Y., 2015. An improved resonance self-shielding calculation method based on equivalence theory. Nucl. Sci. Eng. 179 (3), 233–252.
Zhang, Q., Jiang, R., Zhao, Q., Cao, L., Wu, H., 2018a. Accurate resonance absorption calculation for fuel pins with non-uniform intra-pellet temperature profile based on ultra-fine-group slowing-down calculations. Ann. Nucl. Energy 120, 392–401.
Zhang, Q., Zhao, Q., Yang, W.S., Wu, H., Zhang, Q., Zhao, Q., Wu, H., 2018b. Modeling of resonance-interference effect in depleted fuel compositions by pseudo resonant isotopes. Nucl. Sci. Eng. 191 (1), 46–65.
Zhang, Q., Zhao, Q., Zhang, Z., Liang, L., Yang, W.S., Wu, H., Cao, L., 2018c. Improvements of the embedded self-shielding method with pseudo-resonant isotope model on the multifuel lattice system. Nucl. Sci. Eng., 1–17
Zhang, Q., Zhao, Q., Zhang, Z., Liang, L., Cao, L., Wu, H., 2018d. Investigation on the heterogeneous resonance integral in the embedded self-shielding method. Ann. Nucl. Energy 120, 485–500.